European Journal of Nuclear Medicine and Molecular Imaging
https://doi.org/10.1007/s00259-020-04722-0

ORIGINAL ARTICLE

Imaging CXCR4 expression in patients with suspected primary hyperaldosteronism

Jie Ding[1,2] · Yushi Zhang[3] · Jin Wen[3] · Hui Zhang[4] · Huiping Wang[5] · Yaping Luo[1,2] · Qingqing Pan[1,2] · Wenjia Zhu[1,2] · Xuezhu Wang[1,2] · Shaobo Yao[6] · Michael C. Kreissl[7] · Marcus Hacker[8] · Anli Tong[5] · Li Huo[1,2] · Xiang Li[8]

Received: 5 December 2019 / Accepted: 10 February 2020

Abstract

Purpose It is challenging to differentiate unilateral aldosterone-producing adenoma (APA) from bilateral idiopathic adrenal hyperplasia (IAH) and nonfunctional adrenal adenoma (NFA) in primary aldosteronism (PA). In a first primarily ex vivo study detection, CXC chemokine receptor type 4 (CXCR4) expression has been shown to be a valuable tool for the detection of APA. In this study, we aimed to clinically evaluate CXCR4 imaging with ^{68}Ga-pentixafor PET/CT for detecting APA.

Methods We prospectively recruited 36 patients with clinical suspicion of PA. All patients underwent ^{68}Ga-pentixafor PET/CT. Positive lesions were defined based on higher tracer uptake in adrenal nodular(s) shown on CT than the normal adrenal. These lesions were referred for adrenalectomy subsequently. All patients received clinical follow-up. Semi-quantitative analysis using maximum standardized uptake value (SUV_{max}), lesion-to-liver ratio (LLR), and lesion-to-contralateral ratio (LCR) has also been performed. PET/CT results were correlated with clinical presentation and follow-up.

Results Thirty-nine adrenal lesions in 36 patients were found; 25 APA, 4 IAH, and 10 NFA according to histopathology and clinical assessment. Sensitivity, specificity, and accuracy of ^{68}Ga-pentixafor PET/CT in distinguishing APA by visualization were 100%, 78.6%, and 92.3% respectively. The SUV_{max} of APA (21.34 ± 9.41, $n = 25$) was significantly higher than that of non-APA lesions (6.29 ± 2.10, $n = 14$, $P < 0.0001$). An optimal threshold of $SUV_{max} = 11.18$ was determined for predicting APA with a sensitivity of 88.0%, specificity of 100%, and an accuracy of 92.3%. A cutoff value for LCR of 2.12 yielded a sensitivity of 100% and a specificity of 92.9%, whereas a cutoff value for LLR of 2.36 reached at both 100% of sensitivity and specificity. All patients with (removed) positive lesions benefited from surgery.

Conclusion ^{68}Ga-Pentixafor PET/CT may be used to non-invasively detect APA in PA patients.

Keywords Primary aldosteronism · ^{68}Ga-Pentixafor · CXCR4 · PET/CT

Jie Ding and Yushi Zhang contributed equally to this work.

This article is part of the Topical Collection on Endocrinology

✉ Li Hou
huoli@pumch.cn

✉ Anli Tong
tonganli@hotmail.com

[1] Department of Nuclear Medicine, Peking Union Medical College Hospital, Chinese Academy of Medical Sciences & Peking Union Medical College, Beijing 100730, China

[2] Beijing Key Laboratory of Molecular Targeted Diagnosis and Therapy in Nuclear Medicine, Beijing 100730, China

[3] Department of Urology, Peking Union Medical College Hospital, Chinese Academy of Medical Sciences & Peking Union Medical College, Beijing 100730, China

[4] Department of Pathology, Molecular Pathology Research Center, Peking Union Medical College Hospital, Chinese Academy of Medical Sciences & Peking Union Medical College, Beijing 100730, China

[5] Department of Endocrinology and Key Laboratory of Endocrinology, Ministry of Health, Peking Union Medical College Hospital, Chinese Academy of Medical Sciences & Peking Union Medical College, Beijing 100730, China

[6] Department of Nuclear Medicine, The First Affiliated Hospital of Fujian Medical University, Fuzhou, Fujian 350005, China

[7] Department of Radiology and Nuclear Medicine, University Hospital Magdeburg, Magdeburg, Germany

[8] Division of Nuclear Medicine, Department of Biomedical Imaging and Image-guided Therapy, Medical University of Vienna, Vienna, Austria

Introduction

Primary aldosteronism (PA), also known as primary hyperaldosteronism or Conn's syndrome, is a clinical syndrome with secondary hypertension. It is characterized by the inappropriate elevation of aldosterone levels; aldosterone is autonomously secreted from the adrenal glands and is nonsuppressible with sodium loading [1]. PA is the most common endocrine cause of hypertension [2]. Thus, its early diagnosis and appropriate treatment are essential to minimize its associated risks. Aldosterone-producing adenoma (APA) and idiopathic adrenal hyperplasia (IAH) are the main subtypes of PA [3]. Nonfunctional adrenal adenoma (NFA) is frequently misdiagnosed as APAs [4]. Thus, it is important to distinguish between unilateral and bilateral cases of PA and to categorize PA and NFA.

Non-invasive imaging technologies including computed tomography (CT), magnetic resonance imaging (MRI), and nuclear medicine techniques are commonly used to examine adrenal lesions. Nevertheless, the limited characteristic radiological features on CT and MRI scans can make the detection and characterization of adrenal lesions challenging [5]. Nowadays, adrenal venous sampling (AVS), the best mode of lateralizing PA lesions, is widely accepted in clinical practice [6]. However, AVS is an invasive and technically challenging approach. According to the German Conn's registry, the average rate of successful bilateral AVS is approximately 61%, with a wide variation from 29 to 74% among five centers. Postoperative adrenal bleeding may occur after AVS [7], and the results obtained may be inaccurate [8]. Nuclear medicine functional imaging techniques seem to be able to break this dilemma. Metomidate is an inhibitor of aldosterone synthase (CYP11B2). ^{11}C-Metomidate as a positron emission tomographic (PET) imaging tracer has shown promising results in the characterization of PA patients [9]. Nevertheless, short radio half-life and requirement of an onsite cyclotron could limit clinical use.

The C-X-C chemokine receptor 4 (CXCR4) is a transmembrane G protein-coupled receptor. It was recently demonstrated that the expression of CXCR4 as elevated in aldosterone-producing tissue in APA and its expression is closely associated with the expression of CYP11B2 [10]. CYP11B2 is mainly involved in aldosterone synthesis and can be primarily found in the zona glomerulosa; it is also highly expressed in APA. ^{68}Ga-Pentixafor as a specific radiolabeled CXCR4 ligand has been used in the detection of many hematologic and solid tumors [11]. Recently, it was also used for the detection of APA [10]; in 220 histological samples of adrenal lesions and 2 normal adrenals, CXCR4 expression by immunohistochemistry and quantitative real-time polymerase chain reaction was assessed. A strong expression could be observed and also verified by ^{68}Ga-pentixafor PETCT in 9 patients with known APA. But, there are only few reports on it and still no clinical trials to distinguish the APA and non-APA lesions by 68Ga-pentixafor PET/CT. This study aimed to prospectively evaluate the utility of ^{68}Ga-pentixafor PET/CT in patients with suspected PA, particularly for distinguishing APA from IAH and NFA.

Materials and methods

Study population

We prospectively assessed patients with clinical suspicion of PA at the Peking Union Medical College Hospital. Firstly, unilateral or bilateral adrenal nodule(s) or hyperplasia had been detected on CT scans in these patients. The detailed inclusion criteria of plasma tests for PA were (1) persistent hypertension with blood pressure > 160/100 mmHg or refractory hypertension (blood pressure > 140/90 mmHg with combined use of three types of antihypertensive medications, including diuretics) with hypokalemia, or (2) uncontrollable hypokalemia, with or without hypertension, or (3) persistent hypertension with blood pressure > 160/100 mmHg or refractory hypertension with an aldosterone-to-renin ratio (ARR) ≥ 30 (ng/dl)/(ng/ml/h) (a plasma renin activity < 0.1 ng/ml/h was considered 0.1 ng/ml/h) based on the clinical guidelines subcommittee of the Endocrine Society [1]. Besides, a positive captopril test (a decrease in plasma aldosterone level after captopril administration by ≤ 30%) was regarded as a sufficient but not obligatory condition. In addition, patients who had unilateral or bilateral adrenal nodule(s) with clear border shown on CT but presenting normal serum potassium and ARR < 30 (ng/dl)/(ng/ml/h) have also been included as NFA. The patients who underwent adrenalectomy and had follow-up data were included in our analysis finally. The study protocol was approved by the institutional review board of PUMCH (IRB protocol #ZS-1435). All patients provided written informed consent prior to ^{68}Ga-pentixafor PET/CT. The highest blood pressure, lowest blood potassium level, plasma renin activity, and aldosterone levels were recorded.

^{68}Ga-Pentixafor synthesis

^{68}Ga-Pentixafor was synthesized in a sterile hot cell. The precursor (obtained from CSBio Co., CA, USA) was dissolved in deionized water to 1 mg/ml and stored at 4 °C before use. ^{68}Ga was eluted from an ITG ^{68}Ge/^{68}Ga generator using 0.1 M HCl and mixed with 1.25 M NaOAc buffer to adjust the pH to 4.0. The mixture was then directly transferred to a 1-ml plastic tube containing 20 μg of pentixafor and heated at 100 °C for

10 min. The reaction mixture was then cooled, dissolved in sterile phosphate-buffered saline, and passed through a 0.22 mm aseptic filtration membrane. Thin-layer liquid chromatography (Bioscan, Washington, DC, USA) was used to assess the radiochemical purity, with CH3OH:NH4OAc (1:1 [vol/vol]) as the developing solution. The radiochemical purity of the ^{68}Ga-pentixafor product exceeded 97%.

^{68}Ga-Pentixafor PET/CT scans

All images were obtained using a dedicated PET/CT scanner (PoleStar m660; SinoUnion Healthcare Inc., Beijing, China) at Peking Union Medical College Hospital. Noncontrast CT images were acquired over the region of the adrenals (140 kV, 64 mA, slice width 5 mm). The patients had a normal diet with no special preparation. After 25–30 min of an intravenous injection of ^{68}Ga-pentixafor (61.8 ± 57.0 MBq), PET images of the upper abdomen and adrenal region were acquired over 10 min using one bed position. A three-dimensional ordinary Poisson ordered subset expectation-maximization algorithm, with a point-spread function correction using 2 iterations and 10 subsets, was applied for PET image reconstruction. A 192 × 192 × 117 matrix size and a 3.147 × 3.147 × 1.87 mm^3 voxel size were used. The images were smoothed by means of a 4.5 mm full width at half-maximum Gaussian filter.

Image analysis

Two experienced board-certified nuclear medicine physicians (L. Huo and W. J. Zhu) who were blinded to the clinical information of the patients evaluated the PET/CT data. A positive PET/CT lesion detection was defined by visual analysis: the adrenal nodular(s) shown on CT had higher uptake than that of the ipsilateral and contralateral normal adrenal gland. A negative lesion had an uptake of equal to or less than that of the normal adrenal gland by visual assessment. The maximum standardized uptake values (SUV_{max}) of the adrenal lesions, specific uptake value ratios like the lesion-to-liver ratio (LLR), and lesion-to-contralateral ratio (LCR) were measured by assigning a spherical volume of interest with a diameter of 10 mm to the area of suspicious uptake.

Follow-up assessment

We collected the follow-up data of all postoperative patients more than 3 months after the operation. According to the criteria for assessment of final outcomes established by the Primary Aldosteronism Surgical Outcome study [12], the patients were categorized into three groups: (1) cured: normotensive blood pressure < 140/90 mmHg after surgery without the aid of antihypertensive medication along with normal serum potassium level; (2) improvement: blood pressure reduced, but still ≥ 140/90 mmHg postoperatively with either the same or a lower amount of antihypertensive medication; and (3) no improvement: consistent or increased blood pressure ≥ 140/90 mmHg postoperatively with either the same or an increased amount of antihypertensive medication.

Immunohistochemistry

Immunohistochemical analyses were performed using paraffin-embedded specimens. The antibodies used and their dilutions were as follows: CXCR4 (1:100, ab124824; Abcam) and CYP11B2 (1:100, kindly provided by Dr. Celso E. Gomez-Sanchez, Department of Medicine, University of Mississippi Medical Center). The results of immunohistochemical analyses for CXCR4 and CYP11B2 were evaluated independently by experienced pathologists and expressed as the percentage of positive tumor cells (score 0, no positive cells; score 1, ≤ 10% positive cells; score 2, 10–50% positive cells; score 3, 51–75% positive cells; and score 4, > 75% positive cells).

Non-PET/CT assessment

For comparison with ^{68}Ga-pentixafor PET/CT results, the clinical non-PET criteria for patients were used as detailed below. For the determination of APA, (1) the postoperative pathology was adrenocortical adenoma and (2) positive staining (score, 2–4) of CYP11B2 in adenoma cells. For the determination of IAH, (1) the postoperative pathology was adrenocortical hyperplasia and (2) no or weak CYP11B2 expression (score, 0–1) in hyperplastic cells. For the determination of NFA, (1) the postoperative pathology was adrenocortical adenoma and (2) no or weak CYP11B2 expression (score, 0–1) in adenoma cells. Among PA patients with bilateral adrenal nodules, if the symptoms were alleviated through follow-up after one side of adenoma lesions were resected, the nodules on the contralateral side were assumed to be NFA lesions.

Statistical analysis

Quantitative variables are expressed as means ± standard deviations and ranges. After post hoc testing, the Mann-Whitney *U* test was performed to assess differences between groups. The sensitivity and specificity of ^{68}Ga-pentixafor PET/CT results for an indication of APA, IAH, or NFA lesions were calculated. The correlation between the proportion of CXCR4 positivity and SUV_{max} of adrenal lesions, SUV_{max}, and other characteristics of APA were assessed using the Pearson correlation coefficient. The *P* value between three different follow-up groups was calculated via one-way analysis of variance and chi-square tests. Receiver-operating

characteristic (ROC) curves were constructed to determine the threshold of semi-quantitative parameters and the diagnostic accuracy of ^{68}Ga-pentixafor PET/CT for the diagnosis of APA. The Mann-Whitney *U* test, one-way analysis of variance, and chi-square tests were performed using SPSS version 18 (IBM Corp., Armonk, NY, USA), and the rest of the data were analyzed by GraphPad Prism version 6 (GraphPad Software, San Diego, CA, USA). Analysis items with $P < 0.05$ were considered statistically significant.

Results

Baseline characteristics and clinical management of patients

One patient who was pathologically proven to have a pheochromocytoma was excluded. Thirty-three post-surgical patients who met the PA including criteria and 3 patients who were regarded as the NFA group were included in the final investigation. Twenty-five cases of APA, 3 cases of IAH, and 5 cases of NFA were determined according to the non-PET/CT assessment of the 33 patients who met the PA including criteria. Two cases of NFA and 1 case of IAH were definitely diagnosed in 3 patients in the NFA group. In general, there were 29 PA patients (25 APA and 4 IAH) and 7 NFA patients. The mean age of the 36 patients was 46 ± 10 years. There were 28/29 PA patients with hypertension (96.6%), 21 (75.0%) of which were difficult to control, and 7/21 PA patients with refractory hypertension. Two patients with NFA also had hypertension. Also, 24/29 patients with PA had hypokalemia (82.8%). The ARR among patients with APA and IAH was 173.1 ± 56.9 and 116.4 ± 108.9 (ng/dl)/(ng/ml/h), respectively, which were higher than patients with NFA (82.9 ± 56.8(ng/dl)/(ng/ml/h)). The sensitivity and specificity of ARR = 30 (ng/dl)/(ng/ml/h) to diagnose PA were 96.6% (28/29) and 28.6% (2/7), respectively. Also, 19/21 PA patients (90.5%) showed positive captopril test results. The average length and volume of the lesions were 2.1 cm and 3.9 cm^3 as determined by CT scans. Detailed baseline characteristics are shown in Table 1.

Correlation of ^{68}Ga-pentixafor PET/CT with non-PET/CT clinical diagnoses

There were 39 lesions in 36 patients. Except that 3 APA patients were shown bilateral nodules, the remaining 33 patients were manifested unilateral adrenal gland nodule on CT. All patients underwent unilateral adrenalectomy. A total of 25 APA, 4 IAH, and 7 NFA lesions were confirmed by histology and immunohistochemistry, while the remaining 3 NFA lesions (in the contralateral of APA) were subsequently confirmed via clinical or biochemical follow-up evidence. All of 25 APA lesions showed lateralization results with higher ^{68}Ga-pentixafor uptake than the normal adrenal tissue (Fig. 1). There were no false-negative results among APA lesions. Three IAH and 8 NFA lesions showed comparable ^{68}Ga-pentixafor uptake as the normal adrenal (Fig. 1), while 1 IAH and 2 NFA lesions showed false-positive uptakes (Table 2 and Fig. 2). The sensitivity, specificity, and accuracy of ^{68}Ga-pentixafor PET/CT in distinguishing APA from non-APA lesions by visualization were 100%, 78.6%, and 92.3%, respectively (Table 2).

The ^{68}Ga-pentixafor SUV_{max} of APA (21.34 ± 9.41, $n = 25$) (Fig. 3) was significantly higher than that of non-APA lesions (6.29 ± 2.10, $n = 14$) ($P < 0.0001$). Among non-APA lesions, 4 IAH lesions had a SUV_{max} ranging between 5.16 and 10.83(mean, 7.29), and the SUV_{max} of 10 NFA lesions was 5.31 ± 1.4. An optimal cutoff SUV_{max} value of 11.18 was calculated using the ROC analysis yielding a sensitivity of 88.0% (95% confidence interval [CI], 68.8–97.5), specificity of 100% (95% CI, 76.8–100), and accuracy of 92.3% (95% CI, 79.0–98.1) for the diagnosis of APA (Table 2). The area under the ROC curve was 0.98 (95% CI, 0.94–1.01, $P < 0.0001$). The LCR and LLR of APA lesions were 5.98 ± 0.55 and 6.87 ± 0.77, while those of non-APA lesions were 1.63 ± 0.13 and 1.46 ± 0.13, respectively. There were significant differences in both the LCR and LLR between the two groups ($P < 0.0001$). A cutoff value for LCR of 2.12 yielded a sensitivity of 100% (95% CI, 86.3–100) and a specificity of 92.9% (95% CI, 66.1–99.8), whereas a cutoff value for LLR of 2.36 yielded both a sensitivity (95% CI, 86.3–100) and specificity (95% CI, 76.9–100) of 100%. The areas under the ROC curve for LCR and LLR were 0.99 (95% CI, 0.98–1.01) and 1.00 (95% CI, 1.00–1.00), respectively.

Correlation of ^{68}Ga-pentixafor PET/CT and clinical characteristics with follow-up outcome

We were able to collect the follow-up data of 29 PA patients and 2 symptomatic NFA patients (>3 months and 7.9 ± 3.0 months, respectively) to assess the correlation of ^{68}Ga-pentixafor PET/CT and clinical characteristics with outcomes during follow-up. All patients ($n = 26$) with positive PET lesions benefited from surgical treatment, of which hypertension among 21/26 (80.8%) patients (including 20 APA and 1 IAH) was cured, and the remaining 5/26 (19.2%) patients (5 with APA) showed improvements in hypertension. Of the 5 patients with lesions with no increased uptake, 2 IAH patients obtained improved follow-up findings postoperatively, while 1 IAH and 2 NFA patients did not. The lesions defined by PET/CT

Table 1 Baseline characteristics and therapy management of patients

Characteristics (median, range)	Total ($n = 36$)	APA ($n = 25$)	IAH ($n = 4$)	NFA ($n = 7$)
Age	46 ± 10 (26–66)	44 ± 9 (28–63)	44 ± 14 (26–59)	53 ± 10 (36–66)
Gender (male)	15	10	2	3
Number of hypertension	31	24	4	2
Number of poorly controlled hypertension	22	19	2	1
Duration of hypertension (year)	7.2 ± 5.8 (0.2–20)	7.4 ± 6.0 (0.2–20)	8.5 ± 5.1 (1–12)	2.8 (0.5–5.0)
Systolic pressure (mmHg)	176 ± 29 (115–230)	184 ± 22 (132–230)	186 ± 42 (150–225)	143 ± 23 (115–186)
Diastolic pressure (mmHg)	109 ± 15 (72–140)	113 ± 13 (85–140)	116 ± 19 (100–135)	93 ± 13 (72–110)
Number of hypokalemia	24	21	3	0
Duration of hypokalemia (year)	4.2 ± 5.2 (0.2–18)	4.7 ± 5.4 (0.2–18)	0.8 ± 0.4 (0.3–1)	/
Serum potassium (mmol/l)	2.9 ± 0.9 (1.4–4.6)	2.5 ± 0.7 (1.4–4.0)	3.1 ± 0.7 (2.6–4.1)	4.0 ± 0.4 (3.6–4.6)
Plasma aldosterone concentration (ng/dl)	17.5 ± 5.3 (9.4–30.2)	17.8 ± 5.5 (9.4–30.2)	20.4 ± 3.4 (16.8–24.5)	14.7 ± 4.4 (10.3–23.4)
ARR([ng/dl]/[ng/ml/h])	149.3 ± 72.1 (1.8–301.8)	173.1 ± 56.9 (69.4–301.8)	116.4 ± 108.9 (19.9–245.2)	82.9 ± 56.8 (1.8–145.7)
Number of positive captopril test	19/21	18/20	1/1	/
Lesional location (right)	15	12	0	3
Lesional location (left)	18	10	4	4
Bilateral	3	3	0	0
Tumor length on CT (cm)	2.1 ± 0.7 (1.1–3.8)	2.1 ± 0.6 (1.1–3.8)	1.5 ± 0.2 (1.2–1.7)	2.6 ± 0.7 (1.4–3.8)
Tumor volume on CT (cm^3)	3.9 ± 3.7 (0.5–17.1)	3.4 ± 2.7 (0.5–10.1)	1.0 ± 0.4 (0.5–1.4)	7.4 ± 5.2 (1.0–17.1)

visual analysis (positive uptake/no increased uptake) were highly correlated with hypertension follow-up assessment (cure/improvement/no improvement) among the patients ($\chi^2 = 20.44$, $P = 0.002$). The SUV_{max} of cured patients was higher than that of those who showed improvement or no improvement ($P = 0.02$) (Table 3).

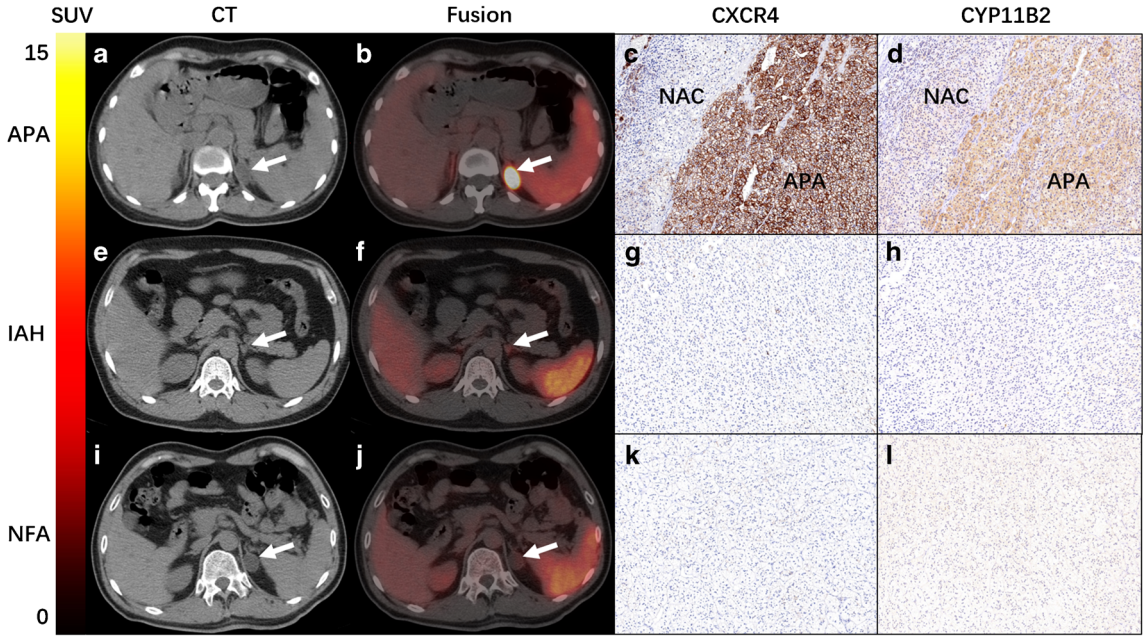

Fig. 1 A–D Representative ^{68}Ga-pentixafor PET/CT of a 44-year-old female patient who presented with general malaise and hypertension. The level of serum potassium was 2.2 mmol/l. A true positive uptake (SUV_{max} 36.4, white arrow) was observed in one APA lesion (adrenocortical adenoma) and NAC normal adrenal cortex with strong expression of CXCR4 and CYP11B2 (C-D). CT demonstrated a 2 × 2.3 cm lesion with intense uptake in the left adrenal gland. The patient's blood pressure and serum potassium returned to normal range after surgery. E–H Representative ^{68}Ga-pentixafor PET/CT of in a 26-year-old male patient. ^{68}Ga-Pentixafor PET/CT was true negative in IAH (adrenal cortex nodular hyperplasia). The lowest serum potassium was 2.7 mmol/l. CT showed left adrenal nodules (1.2 cm) with slightly increased uptake $SUV_{max} = 5.3$. No increased expression of CXCR4 and CYP11B2 was observed by immunochemistry staining. The patient's hypertension persisted after surgery. I–L Representative ^{68}Ga-pentixafor PET/CT: a 44-year-old male showed a true negative NFA lesion. CT visualized a 2.2 cm low-density nodule in the left adrenal gland. No increased uptake was observed in the mass ($SUV_{max} = 5.24$, white arrow). A left adrenocortical adenoma was histopathologically confirmed. The adenoma had no increased CXCR4 and CYP11B2 expression as assessed by immunochemistry staining

Table 2 ^{68}Ga-Pentixafor PET/CT in diagnosis of adrenal gland lesions

^{68}Ga-Pentixafor PET/CT		APA lesions ($n = 25$)	Non-APA lesions ($n = 14$)
Visual analysis	Positive Lesions ($n = 28$)	25 (100%)	3 (21.4%)
	Negative Lesions ($n = 11$)	0 (0%)	11 (78.6%)
Semi-quantitative analysis			
SUV_{max}	≥ 11.18 ($n = 22$)	22 (88.0%)	0 (0%)
	< 11.18 ($n = 17$)	3 (12.0%)	14 (100%)
LCR	≥ 2.12 ($n = 26$)	25 (100%)	1 (7.1%)
	< 2.12 ($n = 13$)	0 (0%)	13 (92.9%)
LLR	≥ 2.36 ($n = 25$)	25 (100%)	0 (0%)
	< 2.36($n = 14$)	0 (0%)	14 (100%)

Correlation of immunohistochemistry findings with the SUV_{max} of ^{68}Ga-pentixafor PET/CT

Thirty-six biopsy samples obtained from 36 patients, including 25 APA, 4 IAH, and 7 NFA lesions, were assessed via immunohistochemistry for CXCR4 and CYP11B2 expression. Twenty-four of 25 APA (96%) lesions showed prominent CXCR4 expression (score, 3–4), and 1/25 (4%) showed moderate expression (score, 2 [50%]). Among 4 IAH and 7 NFA lesions, 5/11 showed negative CXCR4 expression (score, 0), while 6/11 lesions showed slight CXCR4 expression (score, 1). The proportion of CXCR4-positive cells (CXCR4+ cells/total cells) in APA lesions was significantly higher than that among non-APA lesions ($P < 0.0001$) (Fig. 3a). In addition, there was a significant correlation between CXCR4 and CYP11B2 expression ($r = 0.91$, $P < 0.0001$) (Fig. 3c). Additionally, we observed a high correlation between the SUV_{max} of ^{68}Ga-pentixafor PET/CT and the proportion of CXCR4-positive cells ($r = 0.65$, $P < 0.0001$) (Fig. 3d). Besides, the correlation coefficient between the value of ARR and the proportion of CXCR4-positive cells was 0.50($P = 0.002$).

Correlation between clinical characteristics and SUV_{max} in APA

The results of the correlation analyses of SUV_{max} in APA with lesion size, volume, and clinical features among 25 APA patients are shown in Table 1. The correlation coefficients of SUV_{max} obtained were the following: long diameter ($r =$

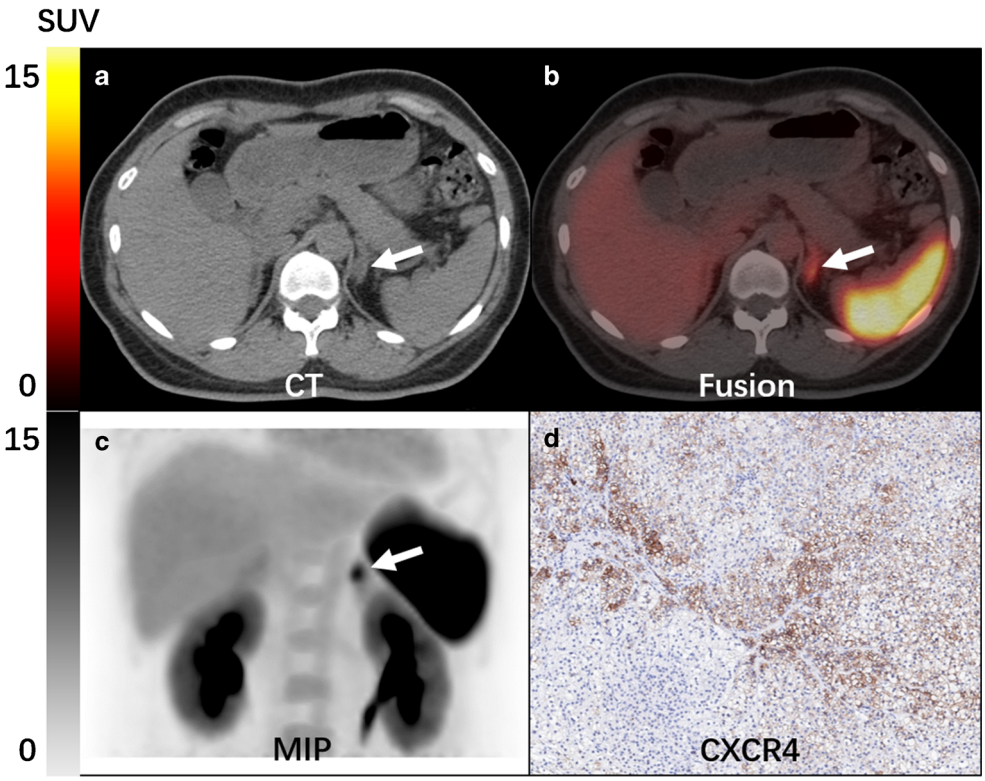

Fig. 2 Representative ^{68}Ga-pentixafor PET/CT scan of a 44-year-old female patient with hypertension showed a false-positive uptake in IAH, and histology approved nodular hyperplasia. A, B Increased activity in the left adrenal nodule with $SUV_{max} = 10.83$ in PET/CT. C MIP map showed foci in the left adrenal area. D CXCR4 prominent expression was observed in adrenal hyperplasia tissue. CYP11B2 immunohistochemistry also revealed the presence of aldosterone-producing cell clusters (APCCs, not shown). Patient's hypertension and hypokalemia abated during 5-month follow-up

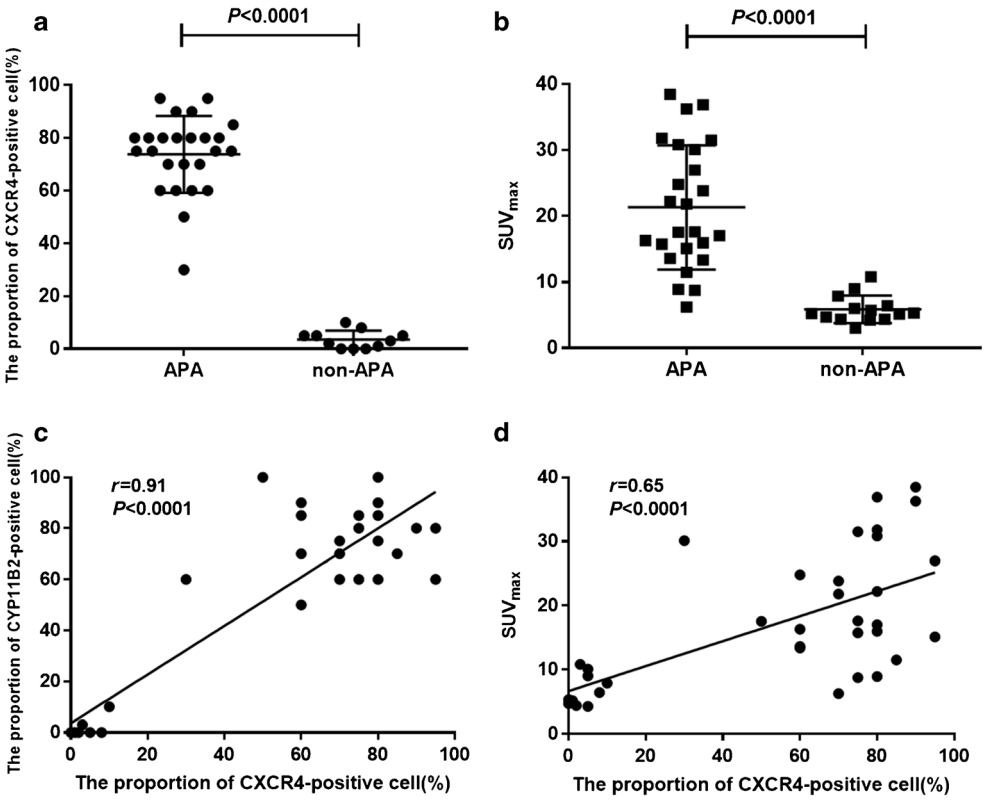

Fig. 3 **a** The proportion of CXCR4-positive cells (%) in APA is significantly higher than non-APA lesions ($P < 0.0001$). **b**. The $SUV_{max} = 21.34 \pm 9.41$ of APA lesions was considerably higher in comparison with non-APA lesions of $SUV_{max} = 6.29 \pm 2.10$. $P < 0.0001$. **c** The scatter diagram showed a significant relationship of CXCR4 expression with CYP11B2 expression (%) ($r = 0.91$, $P < 0.0001$). **d** The significant correlation between ^{68}Ga-pentixafor PET SUV_{max} with CXCR4 expression level ($r = 0.65$, $P < 0.0001$)

0.40, $P = 0.05$), volume ($r = 0.38$, $P = 0.06$), age ($r = -0.34$, $P = 0.10$), systolic pressure ($r = -0.33$, $P = 0.10$), and ARR($r = 0.39$, $P = 0.02$). The correlation coefficients of the other factors were less than 0.3 (Table 4).

Discussion

In the present study, for the first time, the utility of ^{68}Ga-pentixafor PET/CT was prospectively evaluated in patients with suspected PA. Using ^{68}Ga-pentixafor PET/CT, patients were stratified to receive either surgery or follow-up. Histopathological diagnosis served as gold standard, together with follow-up.

Our results prove that ^{68}Ga-pentixafor was a useful and easily implementable technique for the detection of APA lesions. The sensitivity and accuracy of ^{68}Ga-pentixafor PET/CT in distinguishing APA by visualization were 100% and 92.3%, respectively. All APA lesions were recognized by ^{68}Ga-pentixafor PET/CT. However, due to the relatively few negative lesions, the specificity was only 78.6% (11/14). All two false-positive NFA lesions appeared in asymptomatic patients with SUV_{max} values of 6.42 and 9.00. Nevertheless, we only observed a low level of CXCR4 and CYP11B2 expression in the two adrenal nodules. The reason for the false positivity with ^{68}Ga-pentixafor needs to be further investigated.

Regarding the quantitative results of ^{68}Ga-pentixafor PET/CT scan, all APA lesions showed focal ^{68}Ga-pentixafor uptake

Table 3 The comparison of follow-up outcome with ^{68}Ga-pentixafor PET/CT and final diagnosis

	Cure ($n = 21$)	Improvement ($n = 7$)	No Improvement ($n = 3$)	P value
^{68}Ga-Pentixafor PET/CT				
Positive patients ($n = 26$)	21	5	0	< 0.05
Negative patients ($n = 5$)	0	2	3	
SUV_{max}	21.28 ± 9.34	15.77 ± 4.13	4.64 (4.24–5.30)	< 0.05
Final diagnosis				
APA ($n = 25$)	20	5	0	< 0.001
IAH ($n = 4$)	1	2	1	
NFA ($n = 2$)	0	0	2	

$P < 0.05$: statistical significance of the difference in outcome between three groups (cure, improvement, and no improvement)

Table 4 Correlation coefficients between SUV_{max} of APA and clinical characters

Clinical characters	Correlation coefficients	*P* value
Age	−0.34	0.10
Duration of hypertension	−0.21	0.33
Systolic pressure	−0.33	0.10
Diastolic pressure	0.10	0.64
Duration of hypokalemia	−0.23	0.31
Serum potassium	−0.23	0.27
Plasma aldosterone concentration	0.02	0.94
ARR	0.39	0.02
Tumor length on CT	0.40	0.05
Tumor volume on CT	0.38	0.06

with a mean SUV_{max} of 21.34 ± 9.41, which was significantly higher than the mean SUV_{max} (6.29 ± 2.10) identified in non-APA lesions ($P < 0.0001$). A cutoff SUV_{max} value of 11.18 yielded a sensitivity of 88% and a specificity of 100%. The uptake value ratios performed better than SUV, particularly the LLR. When the threshold of LCR was 2.12, the sensitivity and specificity were 100% and 92.86%, respectively. Remarkably, when the cutoff value of LLR was 2.36, both the sensitivity and specificity were 100%. These results suggest that the specific uptake value ratios play a greater role in the differential diagnosis. The proportion of CXCR4 positive cells was significantly correlated with the SUV_{max} of ^{68}Ga-pentixafor PET/CT. Interestingly, the expression of CXCR4 in adenoma cell membrane highly matched the expression of CYP11B2 in the cytoplasm ($r = 9.1$, $P < 0.0001$), which is consistent with the results obtained by Heinze et al. [10]. Pioneering researchers demonstrated that upregulation of mRNA and increased transcription of G protein-coupled receptor caused by hypo-methylation of G protein-coupled receptor-related genes may be the possible reasons of autonomous excess aldosterone production in APA [13], which might be the link of CXCR4 expression and secretion of aldosterone in APA. However, further studies are required to elucidate this hypothesis.

In clinical practice for PA diagnosis, the ARR is widely applied due to its minimal invasiveness and easy serial sampling. However, the ARR is not a reliable testing method with low reproducibility, reporting heterogenetic sensitivities and specificities (range, 66–100% and 61–100%, respectively) [14], and the examination methodology is not yet standardized [15]. In our study, the sensitivity and specificity of ARR ≥ 30 (ng/dl)/(ng/ml/h) to diagnose PA were 96.6% and 28.6%, respectively. The limited number of control group may result in the low specificity. One patient was clinically pre-diagnosed with suspected APA in our research. However, he exhibited no increased adrenal uptake of ^{68}Ga-pentixafor. This lesion was eventually co-defined with NFA by histology immune staining of CYP11B2 and follow-up assessment. Interestingly, another patient was initially suspected of NFA with essential hypertension. ^{68}Ga-Pentixafor PET/CT showed prominent adrenal foci with a SUV_{max} of 16.31. This adrenal adenoma showed a high expression of CYP11B2, and the patient experienced improved hypertension during follow-up. Noticeably, there was positively correction between ARR and the SUV_{max} of ^{68}Ga-pentixafor PET ($r = 0.50$, $P = 0.002$), also between ARR and CXCR4 expression level of adrenal lesions($r = 0.39$, $P = 0.02$).

Conventional imaging modalities, such as CT and MRI, have been widely employed to detect PA lesions in patients younger than 35 years [1]. Nevertheless, with the increasing incidence of NFA among older people, there is a need for functional determination, which is challenging with CT and MRI. A study of 203 patients showed that the detection accuracy of CT was only 53% [16]. ^{68}Ga-Pentixafor could achieve both molecular characterizations of CXCR4 with PA lesions; thus, ^{68}Ga-pentixafor PET/CT possesses a high potential for lesional detection and characterization with relatively high sensitivity and specificity. Particularly, it is helpful for patients whose adrenal lesions are not clearly shown on CT (e.g., slim patients) or ectopic adrenal adenoma. In our study, a PA patient showed a nodule behind the superior vena cava at the level of the renal hilar, which impaired the identification of the right APA on CT. However, the lesion showed prominent uptake on ^{68}Ga-pentixafor PET/CT. Besides, ^{68}Ga-pentixafor PET/CT also showed a unique advantage for patients with bilateral adrenal lesions (Fig. 4).

^{131}I-Iodomethyl-norcholesterol (NP-59) SPECT has been used in the diagnosis of PA patients [17], but it is no longer widely used because of the tedious examination process and low spatial resolution. ^{11}C-Metomidate is an inhibitor of 11-hydroxylase (CYP11B1) and CYP11B2 [18]. Burton et al. [19] studied 39 PA patients and 5 NFA patients and reported a SUV_{max} of ^{11}C-metomidate in APA patients as 21.7 ± 1.6, which was significantly higher than that of normal adrenal tissues ($SUV_{max} = 13.8 \pm 0.6$, $P = 0.00003$). The SUV_{max} (^{11}C-metomidate) of nonfunctional adenomas and bilateral adrenal lesions was 11.5 ± 3.3 and 17.3 ± 1.2, respectively. The sensitivity and specificity of a cutoff SUV_{max} ratio of 1.25 (tumor to normal adrenal) in the diagnosis of APA were 76% and 87%, and a specificity of 100% was achieved with a $SUV_{max} \geq 17$. Our study showed that when the cutoff value of the LLR was 2.36, both the sensitivity and specificity of ^{68}Ga-pentixafor for differentiating between APA and non-APA lesions were 100%. LCR reached a sensitivity and specificity of 100% and 92.86%, respectively, when the ratio was 2.12.

The diagnostic performance SUV (^{11}C-metomidate) of APA reported comparable results with SUV (^{68}Ga-pentixafor). However, the miscellaneous uptake of ^{11}C-metomidate in IAH and NFA could limit the clinical application. Moreover, the synthesis of ^{11}C-metomidate requires a

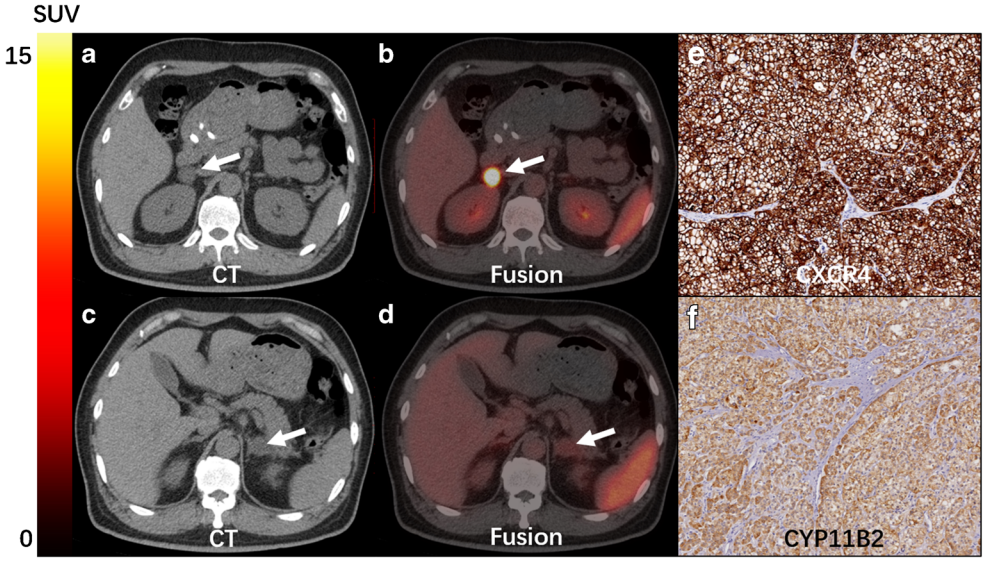

Fig. 4 Representative ^{68}Ga-pentixafor PET/CT of a 55-year-old male patient; the scans distinguished unilateral APA form bilateral adrenal nodules. Bilateral adrenal nodules were detected by CT (right 2.1 cm, left 2.6 cm). A, B CT and fusion images revealed significantly increased activity at right adrenal lesion with SUV_{max} = 30.86. C, D CT and PET/CT images showed a slight radioactivity uptake in the left adrenal nodule with SUV_{max} = 3.0. The patient underwent right adrenal tumor resection, which was proven adrenocortical adenoma pathologically. E, F The results of CXCR4 and CYP11B2 immunohistochemistry represented significantly high expression in the adenoma cell membrane and cytoplasm, respectively. The patient's hypertension was cured after surgery; the lesion on the left side was diagnosed as a nonfunctional nodule by follow-up

large cyclotron, and the 20 min half-life of ^{11}C-metomidate could limit its clinical use. Also, oral low-dose dexamethasone before ^{11}C-metomidate PET examination is required to inhibit the activity of CYB11B1 enzyme in the normal adrenal gland to reduce the uptake of the tracer [19, 20]. But, the patients did not need special preparation before ^{68}Ga-pentixafor PET/CT examination. All in all, according to our data, ^{68}Ga-pentixafor-targeted imaging seems to be more superior and convenient compared with ^{11}C-methionine in the detection of APA lesions. However, a head-to-head comparison is needed to assess if the method is indeed preferred. ^{123}I-Iodometomidate SPECT has been used in adrenocortical tumors for functional characterization and treatment decisions [21, 22]. Hahner et al. [22] found a significant uptake of ^{123}I-iodometomidate in APA lesions which indicates that it was a promising inspection method for PA patients. However, based on the fact that PET has a higher spatial resolution than SPECT, for some small lesions, ^{68}Ga-pentixafor might have a higher sensitivity than ^{123}I-iodometomidate.

The visualization results of ^{68}Ga-pentixafor PET/CT were closely related to post-surgical outcomes. All PA patients with positive uptake lesions (n = 26) benefitted from adrenalectomy, of which 80.8% (21/26) patients were cured. None of 5 negative patients had been cured and 3 of them had no improvement in postoperative symptoms. One IAH patient who showed a focal uptake on the right adrenal area with SUV_{max} = 10.83 (Fig. 2) was cured after unilateral adrenalectomy. Based on the results of CYP11B2 and CXCR4 immunohistochemistry, the positive IAH lesions in ^{68}Ga-pentixafor PET/CT might reveal the presence of aldosterone-producing cell clusters, which are clusters of cells secreting aldosterone and the leading cause of hypertension and hypokalemia [23]. Thus, ^{68}Ga-pentixafor PET/CT might be a highly promising approach to reveal the expression of functional lesions and to guide surgery. We also found that the SUV_{max} of ^{68}Ga-pentixafor does not correlate with clinical characteristics and tumor diameters or volumes intensely, which means that ^{68}Ga-pentixafor PET/CT had good repeatability.

This unicentric prospective study has two limitations. Firstly, the limited number and unbalanced patient cohort in our study might lead to biased results. Secondly, limited AVS data were obtained for correlation with this ^{68}Ga-pentixafor study. However, we used patients' follow-up results as ground evidence for reference.

Conclusions

In this prospective study, SUV_{max} of PA in ^{68}Ga-pentixafor PET/CT was firmly related to the molecular expression of CXCR4 and CYP11B2. ^{68}Ga-Pentixafor PET/CT is a highly sensitive and specific non-invasive approach for PA localization and characterization.

Acknowledgments We are grateful to Dr. Celso E. Gomez-Sanchez (Department of Medicine, University of Mississippi Medical Center, Jackson, Mississippi), who kindly provided us antibodies against CYP11B2.

Funding information This work was sponsored in part by the National Natural Science Foundation of China (Grant No. 81571713), CAMS Innovation Fund for Medical Sciences (CIFMS). Grant No. 2016-I2M-4-003, CAMS initiative for innovative medicine (No. CAMS-2018-I2M-3-001). The National Natural Science Foundation of China (81601529), the Tianjin Natural Science Foundation (18JCQNJC11600).

Compliance with ethical standards

Conflict of interest SCINTOMICS owns the IP on Pentixafor. All other authors declare that they have no conflict of interest.

Ethical approval The clinical institutional review board approved this study.

References

1. Funder JW, Carey RM, Mantero F, Murad MH, Reincke M, Shibata H, et al. The management of primary aldosteronism: case detection, diagnosis, and treatment: an Endocrine Society Clinical Practice Guideline. J Clin Endocrinol Metab. 2016;101(5):1889–916.
2. Monticone S, D'Ascenzo F, Moretti C, Williams TA, Veglio F, Gaita F, et al. Cardiovascular events and target organ damage in primary aldosteronism compared with essential hypertension: a systematic review and meta-analysis. Lancet Diabetes Endocrinol. 2018;6(1):41–50.
3. Monticone S, Burrello J, Tizzani D, Bertello C, Viola A, Buffolo F, et al. Prevalence and clinical manifestations of primary aldosteronism encountered in primary care practice. J Am Coll Cardiol. 2017;69(14):1811–20.
4. Li LL, Gu WJ, Dou JT, Yang GQ, Lv ZH, et al. Incidental adrenal enlargement: an overview from a retrospective study in a Chinese population. Int J Endocrinol. 2015;2015:192874.
5. Nanba AT, Nanba K, Byrd JB, Shields JJ, Giordano TJ, Miller BS, et al. Discordance between imaging and immunohistochemistry in unilateral primary aldosteronism. Clin Endocrinol. 2017;87(6):665–72.
6. Rossi GP. Update in adrenal venous sampling for primary aldosteronism. Curr Opin Endocrinol Diabetes Obes. 2018;25(3):160–71.
7. Okamura K, Okuda T, Shirai K, Abe I, Kobayashi K, Ishii T, et al. Persistent primary aldosteronism despite iatrogenic adrenal hemorrhage after adrenal vein sampling. J Clin Med Res. 2018;10(1):66–71.
8. Layden BT, Hahr AJ, Elaraj DM. Primary hyperaldosteronism: challenges in subtype classification. BMC Res Notes. 2012;5:602.
9. Powlson AS, Gurnell M, Brown MJ. Nuclear imaging in the diagnosis of primary aldosteronism. Curr Opin Endocrinol Diabetes Obes. 2015;22(3):150–6.
10. Heinze B, Fuss CT, Mulatero P, Beuschlein F, Reincke M, Mustafa M, et al. Targeting CXCR4 (CXC chemokine receptor type 4) for molecular imaging of aldosterone-producing adenoma. Hypertension. 2018;71(2):317–25.
11. Walenkamp AME, Lapa C, Herrmann K, Wester HJ. CXCR4 ligands: the next big hit? J Nucl Med. 2017;58(Suppl 2):77S–82S.
12. Williams TA, Lenders JWM, Mulatero P, Burrello J, Rottenkolber M, Adolf C, et al. Outcomes after adrenalectomy for unilateral primary aldosteronism: an international consensus on outcome measures and analysis of remission rates in an international cohort. Lancet Diabetes Endocrinol. 2017;5(9):689–99.
13. Itcho K, Oki K, Kobuke K, Yoshii Y, Ohno H, Yoneda M, et al. Aberrant G protein-receptor expression is associated with DNA methylation in aldosterone-producing adenoma. Mol Cell Endocrinol. 2018;461:100–4.
14. O'Shea PM, Griffin TP, Denieffe S, Fitzgibbon MC. The aldosterone to renin ratio (ARR) in the diagnosis of primary aldosteronism (PA): promises and challenges. Int J Clin Pract. 2019;73(7):e13353.
15. Käyser SC, Dekkers T, Groenewoud HJ, van der Wilt GJ, Carel Bakx J, van der Wel MC, et al. Study heterogeneity and estimation of prevalence of primary aldosteronism: a systematic review and meta-regression analysis. J Clin Endocrinol Metab. 2016;101(7):2826–35.
16. Young WF, Stanson AW, Thompson GB, Grant CS, Farley DR, van Heerden JA. Role for adrenal venous sampling in primary aldosteronism. Surgery. 2004;136(6):1227–35.
17. Yen RF, Wu VC, Liu KL, Cheng MF, Wu YW, Chueh SC, et al. 131I-6beta-iodomethyl-19-norcholesterol SPECT/CT for primary aldosteronism patients with inconclusive adrenal venous sampling and CT results. J Nucl Med. 2009;50(10):1631–7.
18. Wang T, Satoh F, Morimoto R, Nakamura Y, Sasano H, Auchus RJ, et al. Gene expression profiles in aldosterone-producing adenomas and adjacent adrenal glands. Eur J Endocrinol. 2011;164(4):613–9.
19. Burton TJ, Mackenzie IS, Balan K, Koo B, Bird N, Soloviev DV, et al. Evaluation of the sensitivity and specificity of (11)C-metomidate positron emission tomography (PET)-CT for lateralizing aldosterone secretion by Conn's adenomas. J Clin Endocrinol Metab. 2012;97(1):100–9.
20. Mendichovszky IA, Powlson AS, Manavaki R, Aigbirhio FI, Cheow H, Buscombe JR, et al. Targeted molecular imaging in adrenal disease-an emerging role for metomidate PET-CT. Diagnostics (Basel). 2016;6(4). https://doi.org/10.3390/diagnostics6040042.
21. Kreissl MC, Schirbel A, Fassnacht M, Haenscheid H, Verburg FA, Bock S, et al. [(1)(2)(3)I]Iodometomidate imaging in adrenocortical carcinoma. J Clin Endocrinol Metab. 2013;98(7):2755–64.
22. Hahner S, Kreissl MC, Fassnacht M, Haenscheid H, Bock S, Verburg FA, et al. Functional characterization of adrenal lesions using [123I]IMTO-SPECT/CT. J Clin Endocrinol Metab. 2013;98(4):1508–18.
23. Nanba K, Tsuiki M, Sawai K, Mukai K, Nishimoto K, Usui T, et al. Histopathological diagnosis of primary aldosteronism using CYP11B2 immunohistochemistry. J Clin Endocrinol Metab. 2013;98(4):1567–74.